Journal of ELECTRONIC MATERIALS, Vol. 48, No. 9, 2019
https://doi.org/10.1007/s11664-019-06924-1

Protective Properties of Electrochemically Deposited Al-Based Coatings on $Yb_{0.3}Co_4Sb_{12}$ Skutterudite

XIN BAO,[1,2] MING GU,[2] QIHAO ZHANG,[2] ZIHUA WU,[1] SHENGQIANG BAI,[2,3] LIDONG CHEN,[2] and HUAQING XIE[1,4]

1.—School of Environmental and Materials Engineering, Shanghai Polytechnic University, Shanghai 201209, China. 2.—State Key Laboratory of High Performance Ceramics and Superfine Microstructure, Shanghai Institute of Ceramics, Chinese Academy of Sciences, Shanghai 200050, China. 3.—e-mail: bsq@mail.sic.ac.cn. 4.—e-mail: hqxie@sspu.edu.cn

To protect $CoSb_3$-based skutterudite thermoelectric materials from oxidation and to suppress the sublimation of antimony in long-time service, a series of surface coatings including Al, Al-Ni, Al-Ni-Al were deposited onto $Yb_{0.3}Co_4Sb_{12}$ by using an electrochemical deposition method. The thermal aging behavior for the $Yb_{0.3}Co_4Sb_{12}$ samples with and without different surface coatings were investigated by accelerated thermal aging tests at 873 K. Thermoelectric properties of $Yb_{0.3}Co_4Sb_{12}$ with different coatings after aging are used as the evaluation criteria for coating effectiveness. After thermal aging at 873 K for 30 days, the thermoelectric properties of $Yb_{0.3}Co_4Sb_{12}$ coated with Al-Ni double-layered coating were almost undecreased, indicating that the Al-Ni coating is suitable for protecting $CoSb_3$-based skutterudite from oxidation and for suppressing the sublimation of antimony. It is expected that this coating could improve the reliability of $CoSb_3$-based devices and could accelerate the application of skutterudite thermoelectric generators.

Key words: Thermoelectric, coating, electrochemical deposition, $CoSb_3$-based skutterudite

INTRODUCTION

Thermoelectric (TE) materials can directly convert heat into electric power using the Seebeck effect, and so have potential application in waste heat recovery. The theoretical conversion efficiency of TE materials depends on the dimensionless figure of merit, $ZT = S^2\sigma T/\kappa$, where S is the Seebeck coefficient, σ is the electrical conductivity, T is the absolute temperature, and κ is the total thermal conductivity. In the past 20 years, great progress has been made in the improvement of TE properties. $CoSb_3$-based skutterudites (SKDs) have been regarded as one of the most promising TE materials in the medium temperature range.[1–3] The ZT values of filled skutterudites have been greatly improved to 1.7–2.0[4,5] and the theoretical conversion efficiency for these TE materials has reached above 15%. However, $CoSb_3$-based SKD is faced with the problem of degradation in TE properties at high temperatures due to oxidation, thermal decomposition and the sublimation of antimony.[6,7] The troublesome oxidation can completely incapacitate the TE element in a short service period, and decomposition by sublimation of Sb atoms can change the composition of TE materials and eventually result in the degradation of the TE performance. Moreover, the sublimation products can diffuse or condense on the cold side of TE unicouples, leading to electrical shorts in the TE device.[8] To increase their reliability and to prolong the service life of SKD-based TE modules, it is desirable to develop a protective coating to prevent both oxidation and sublimation. There have been some studies about the coatings for $CoSb_3$-based SKDs. El-Genk et al.[9,10] found that the metal coatings of Mo, V, Ta, and Ti can effectively suppress the sublimation of Sb in $CoSb_3$-based SKDs. Godlewska et al.[11] deposited a Cr-5Si thin

(Received July 5, 2018; accepted January 3, 2019; published online January 11, 2019)

film coating onto $CoSb_3$ using pulse magnetron sputtering, preventing the oxidation of SKDs in high-temperature air, but the thin film coatings lost the protection ability at 600°C. Zhao et al.[12] deposited a Ti coating on the $CoSb_3$ substrate by DC magnetron sputtering to prevent the sublimation of Sb. The coated $CoSb_3$ sample with thicker Ti film had lower weight loss per unit area after accelerated thermal aging tests at 650°C. Compared with the uncoated $CoSb_3$ material, the degradation of TE properties of coated $CoSb_3$ slowed down. Afterward, Dong et al.[13,14] fabricated inorganic–organic silica based composite protective coatings dispersed with glass or granular alumina particles for SKDs via a modified sol–gel procedure combined with a slurry-blade method. The results showed that the formation of micro-cracks was restrained by either glass particles or alumina particles during solidification due to the relaxation of tremendous cohesive stresses in the gel. After thermal aging at 600°C in vacuum, inter-diffusion of Sn from the glass to SKDs and of Sb from SKDs to the coating layer was observed in the silica-based composite coatings with dispersed glass particles. Above all, the previous studies of metal coatings have shown effective suppression of oxidation and Sb-sublimation. However, most of the metal films coated by magnetron sputtering do not have strong bonding with the SKDs. Meanwhile, the coatings were easy to crack or could readily fall off of the TE substrate after long-time thermal aging or thermal cycling. On the other hand, composite coatings consisting of non-metallic materials are complex to obtain and the thickness of protective films is difficult to control.

In this study, three kinds of coatings (Al, Al-Ni, and Al-Ni-Al coatings) were electroplated on the $Yb_{0.3}Co_4Sb_{12}$ substrate to prevent the oxidation and the sublimation of Sb. Accelerated thermal aging tests were conducted on the samples with different coatings at 873 K for different times. The microstructures of the interfaces and thermal aging behaviors of different coatings were investigated by scanning electron microstructure (SEM). The effects of different coatings on preventing the oxidation of $CoSb_3$-based SKDs and suppressing the sublimation of Sb were assessed by evaluating the TE properties of the samples before and after thermal aging. It is expected that these results could facilitate the study of reliability of $CoSb_3$-based devices and accelerate the application of skutterudite TE generators.

EXPERIMENTAL PROCEDURE

$Yb_{0.3}Co_4Sb_{12}$ powders were synthesized by melting, quenching, and annealing processes. Stoichiometric quantities of the constituent pure elements Co (99.97%, powder), Sb (99.99%, powder) and Yb (99%, powder) were weighed according to the mole ratio, loaded into graphite crucibles in a quartz tube, and sealed under a pressure of 0.1 Pa in an argon atmosphere. Then, the samples were melted at 1373 K for 12 h, followed by quenching in saltwater. After annealing at 933 K for 168 h, the ingots were ground into fine powders and sieved to get $Yb_{0.3}Co_4Sb_{12}$ powders. The powders were loaded into graphite dies of diameter 30 mm and sintered at 620–640°C under pressure of 55-60 MPa in flowing argon by hot-pressing (HP) sintering.[15,16] The sintered wafers were cut into 3 mm × 3 mm × 9 mm cuboids and Φ10 mm × 2 mm cylinders by wire cut electrical discharge machining (WEDM). All $Yb_{0.3}Co_4Sb_{12}$ samples had a relative density of over 97% estimated via the Archimedes method.

An electroplating technique was used to deposit Al, Al-Ni and Al-Ni-Al coatings on the $CoSb_3$-based SKD substrate. Before plating, the surface of all samples required pretreatment. The surfaces of the samples were carefully polished. To remove organic impurities, the samples were rinsed in an alkaline degreasing agent at 40°C for 3 min and then washed with deionized water. To remove inorganic impurities and surface oxides, all the samples were etched in a HNO_3:HF:H_2O = 3:1:6 mixed solution for 40 s, and then cleaned with deionized water. Tables I and II present the composition of the electroplating bath and plating parameters. The thicknesses of various coatings could be controlled by adjusting the electrodeposition time and the current density. Figure 1 shows the diagrammatic sketch of various coatings.

All the surfaces of the bar-shaped SKD samples were coated with single- or multi-layer metal coatings. The surface morphology of different coatings on the SKD substrates were characterized by field emission SEM (JSM-6700F, JEOL). The samples with different coatings (Al, Al-Ni, Al-Ni-Al) were put into a quartz tube without sealing, heated to 873 K in the furnace in air and then kept at this temperature for 5 days, 10 days, 15 days and 30 days in order to investigate their isothermal aging behavior. All samples were naturally cooled down to room temperature in the furnace. The compositions of different coatings after thermal aging were identified by energy dispersive spectroscopy (EDS) and x-ray diffraction (XRD, Rigaku, Rint-2000).

The Seebeck coefficient and electrical conductivity were simultaneously measured using a ZEM-3 (ULVACRIKO, Japan) under a helium atmosphere. The uncertainty of the electrical resistivity and Seebeck coefficient measurements is around 5%. The measurement of thermal conductivity was

Table I. Composition of electroplating aluminum bath and plating parameters

$C_8H_{15}N_2Cl$	300 g/L
$AlCl_3$	200 g/L
C_6H_6	450 g/L
Current density	15–20 mA/cm^2
Plating temperature	59°C

carried out by a laser flash method (NETZSCH, LFA457) in a flowing Ar atmosphere. The thermal conductivity (κ) was calculated by $\kappa = D \times C_p \times \rho$, where D is the thermal diffusivity measured by the laser flash technique (LFA 457, Netzsch, Germany), C_p is the specific heat measured on a differential scanning calorimeter (DSC, 204F1, Netzsch, Germany), and ρ is the density measured by the Archimedes method. The uncertainty of κ is estimated to be within 5%, considering the uncertainties for D, C_p and ρ. All TE properties were measured in the temperature range of 300–850 K.

RESULTS AND DISCUSSION

Figure 2 shows the electrical performances of the uncoated $Yb_{0.3}Co_4Sb_{12}$ as a function of thermal aging time at 873 K. The electrical conductivity (σ) shown in Fig. 2a is obviously decreased after thermal aging at 873 K. It can be seen that with the extension of the aging time, the σ shows a decreasing trend at all measurement temperatures in the range from 300 K to 850 K. After accelerated thermal aging for 30 days, the measured σ of uncoated $Yb_{0.3}Co_4Sb_{12}$ at 850 K decreases by about 30%. Figure 2b shows the Seebeck coefficient (S) of the uncoated $Yb_{0.3}Co_4Sb_{12}$ sample after the 873 K-thermal-aging test. It can be seen that the Seebeck coefficient shows little change with the aging time. The key point to evaluating the changes in the electrical conductivity of $CoSb_3$ lies in the change of composition due to the sublimation of Sb and oxidation at high temperature.[17] The sublimation of antimony in $CoSb_3$ sample follows the equation[18]: $CoSb_3 = CoSb_2 + Sb$ (g). The oxidation products of $Yb_{0.3}Co_4Sb_{12}$ are composed of Yb_2O_3, Sb_2O_3, a-Sb_2O_4, b-Sb_2O_4, $CoSb_2O_4$ and so on.[19] All of these could lead to deterioration of the TE properties of the $CoSb_3$-based material, especially the electrical conductivity.

Table II. Composition of electroplating nickel bath and plating parameters

$Ni(NH_2SO_3)_2{\cdot}6H_2O$	300 g/L
H_3BO_3	35 g/L
Current density	10–20 mA/cm^2
Plating temperature and time	35°C (30 min)

Figure 3 shows the surface microscopic morphology of various protective coatings on the $Yb_{0.3}Co_4Sb_{12}$ substrate. In Fig. 3a, it can be seen that there are a few cracks, pores or other defects within the Al coating. Compared to the Al coating, the Al-Ni and Al-Ni-Al coatings show more smooth and dense microscopic morphology. The key point of the DC deposition process is the formation of a new nucleus and the growth of the crystal particle, which directly affects the size of the crystal for the coating.[20] The thickness of the coatings can be controlled by the current density and the deposition time.

Figure 4 shows the fractural surface microscopic morphology of the $Yb_{0.3}Co_4Sb_{12}$ substrate with different coatings deposited by electroplating. Figure 4a shows the morphology of the as-prepared $Yb_{0.3}Co_4Sb_{12}$ with Al coating before aging. The Al coating looks with lots of cracks and micropores. After aging at 873 K for 15 days, there is newly-built interlayers between the Al coating and

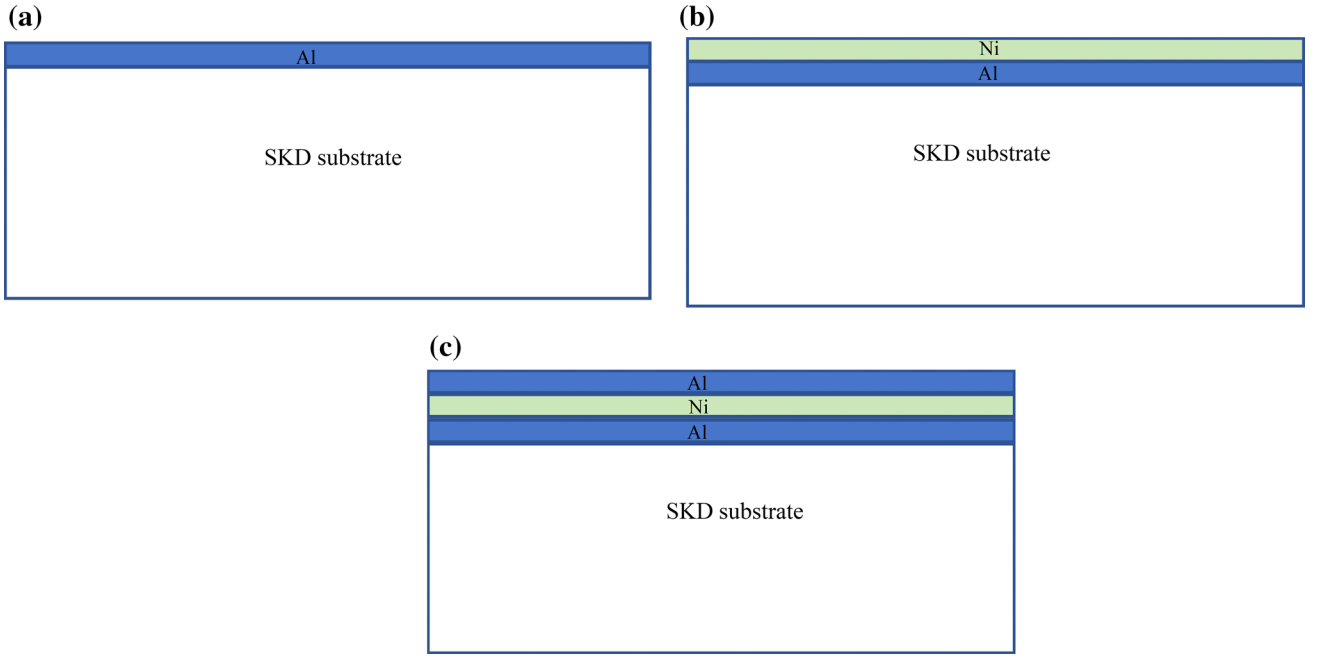

Fig. 1. Schematic diagram of Al (a), Al-Ni (b), and Al-Ni-Al (c) coatings on skutterudite.

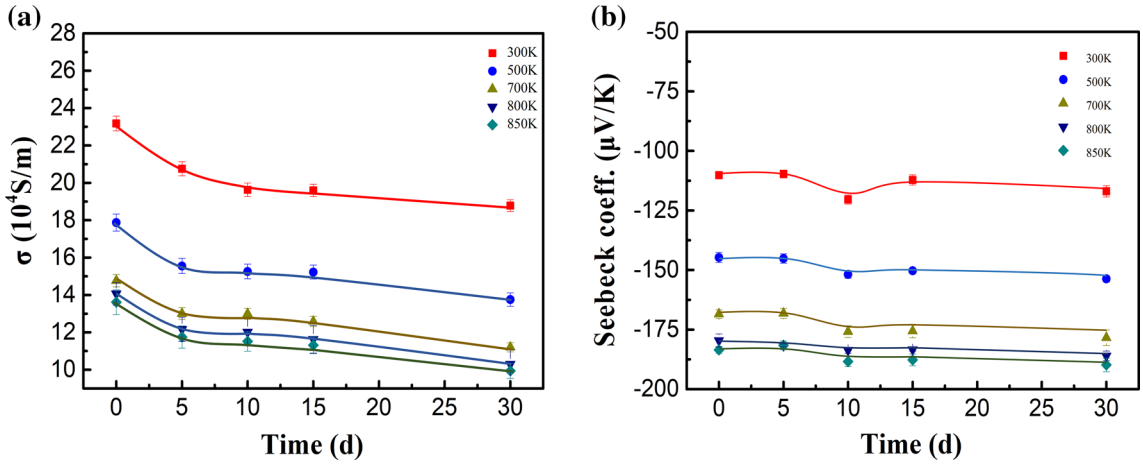

Fig. 2. Electrical performances of uncoated $Yb_{0.3}Co_4Sb_{12}$ as a function of thermal aging time at 873 K. (a) electrical conductivity; (b) Seebeck coefficient.

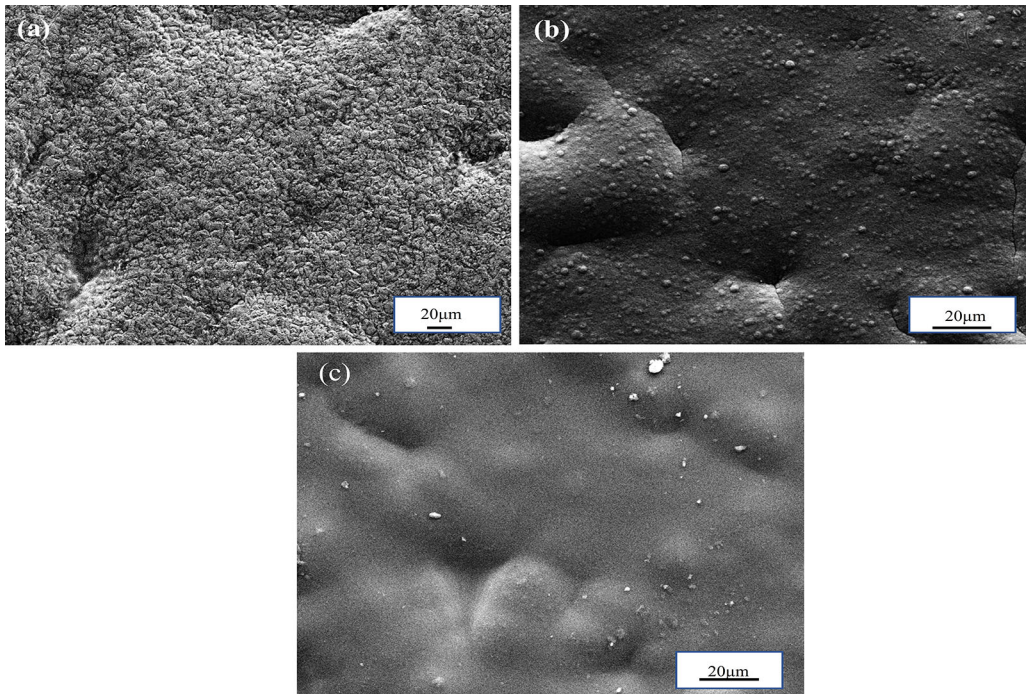

Fig. 3. Surface morphologies of different coatings on $Yb_{0.3}Co_4Sb_{12}$ substrate using DC electrochemical deposition. (a) Al coating, (b) Al-Ni coating, (c) Al-Ni-Al coating.

$Yb_{0.3}Co_4Sb_{12}$ substrate, as shown in Fig. 4b. According to Table III, the main phase of the interlayer is $CoSb_2O_4$, which should be caused by the oxidation. Comparing zone A with zone B in the newly-built oxidation layer of Fig. 4b, it can be observed that the Al coating has the ability to retard the oxidation process. The oxidation in zone B of Fig. 4b is more severe, probably due to the deficiency of the Al coating in this zone. As shown in Fig. 4c and e there is no diffusion between Al and Ni. Figure 4d and f shows the fractural morphologies of the $Yb_{0.3}Co_4Sb_{12}$ substrate with Al-Ni coating and Al-Ni-Al coating after aging at 873 K for 15 days, respectively. Clearly, there is no new phase between the coating and the substrate, indicating that Al-Ni coating and Al-Ni-Al coating effectively prevented the oxidation of the $Yb_{0.3}Co_4Sb_{12}$ substrate. The thickness of the Al-Ni coating is about 27 μm and the thickness of the Al-Ni-Al coating is about 42 μm.

Figure 5 shows the line scanning results of the fractural morphology of different coatings on the $Yb_{0.3}Co_4Sb_{12}$ substrate after thermal aging at 873 K for 15 days. The composition analysis and line scanning results in Fig. 5a confirm that the sole Al

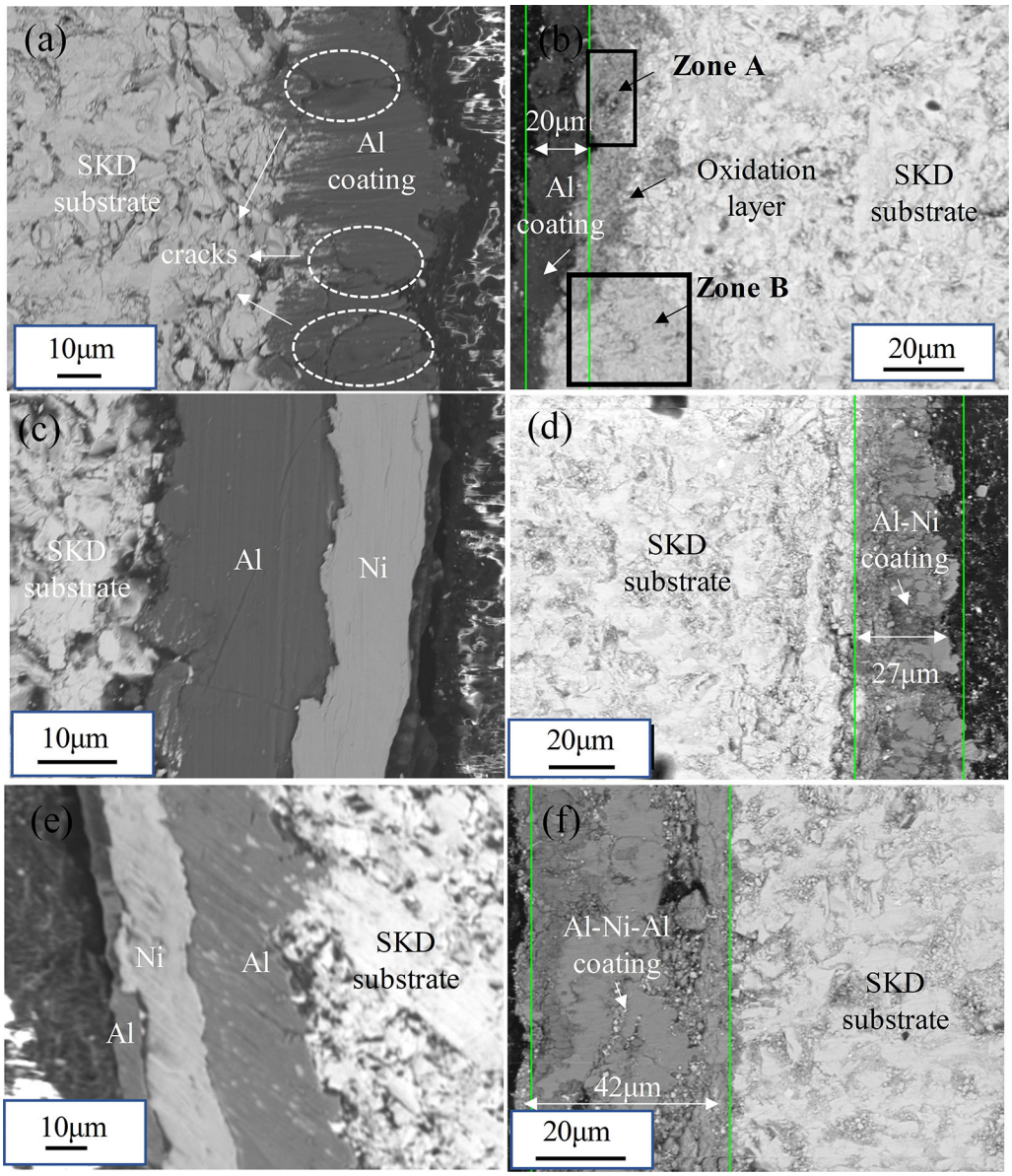

Fig. 4. Fractural morphologies of different coatings on $Yb_{0.3}Co_4Sb_{12}$ substrate using DC electrochemical deposition after thermal aging at 873 K for different times: (a) Al coating, 0 day, (b) Al coating, 15 days, (c) Al-Ni coating, 0 day, (d) Al-Ni coating, 15 days, (e) Al-Ni-Al coating, 0 day, (f) Al-Ni-Al coating, 15 days.

Table III. A summary of the interlayer phase between Al coating and SKD substrate in Fig. 4b measured by the EDS technique

Element	at.%
O	47.71
Co	15.35
Sb	36.02
Yb	0.74
Total	100.00

coating cannot prevent oxidation. The oxide thickness within the substrate is about 55–70 μm after thermal aging for 15 days. As for the Al-Ni- and Al-Ni-Al-coated samples, aluminum and nickel have diffused mutually to form ordered intermetallic compounds during the high-temperature thermal aging test. The compounds may consist of Al_3Ni, AlNi, $AlNi_3$, Al_3Ni_2, and Al_3Ni_5.[21–23] Moreover, according to Fig. 6, we find that antimony cannot be observed in the coatings. The Al, Al-Ni, and Al-Ni-Al coatings have the ability to suppress the sublimation of antimony.

Figure 7 shows the XRD patterns of various coatings on the $Yb_{0.3}Co_4Sb_{12}$ substrate after aging at 873 K for 15 days. It can be observed that the strongest diffraction peak of the Al coating is located at about $2\theta = 45.2°$, which corresponds to Al_2O_3. Some impurity peaks of AlSb are also found. The

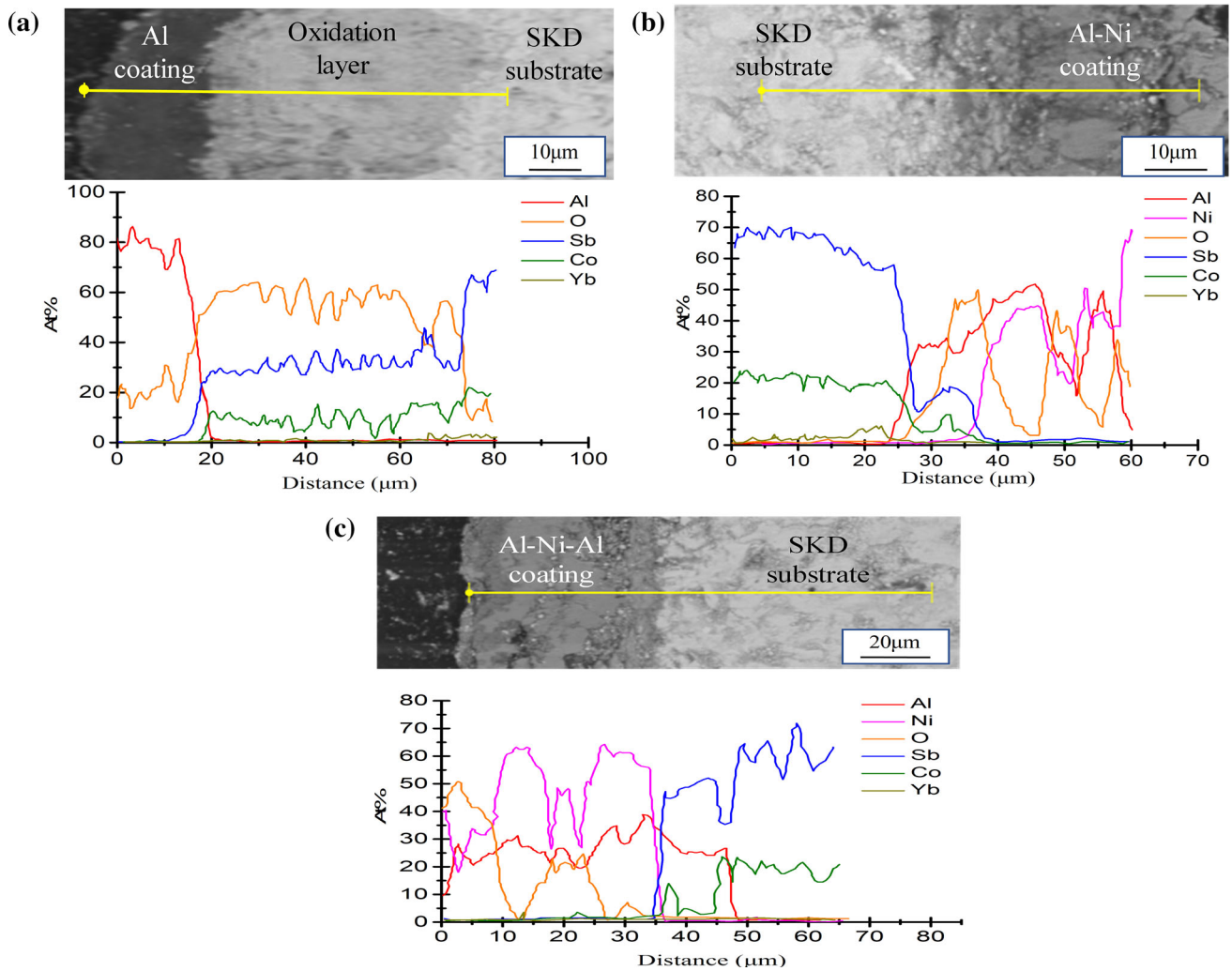

Fig. 5. Line scanning of the fractural morphologies of different coatings on $Yb_{0.3}Co_4Sb_{12}$ substrate after thermal-aging at 873 K for 15 days. (a) Al coating, (b) Al-Ni coating, (c) Al-Ni-Al coating.

main peaks of the Al-Ni coating and the Al-Ni-Al coating are located at about $2\theta = 44.9°$. Combined with the EDS analysis of the Al-Ni diffusion layer, it is determined that the main peak at 44.9 degree is mainly $AlNi_3$, Al_2Ni_5 and Al-Ni oxidation. The contents of the Al-Ni diffusion layer analyzed by EDS technology are shown in Table IV.

Figure 8 presents the TE properties of $Yb_{0.3}Co_4Sb_{12}$ samples after accelerated thermal aging testing. To avoid the influence of the coating on the TE properties, all coated samples subjected to thermal aging were characterized after removing the coatings. It can be seen from Fig. 8a that the σ of uncoated $Yb_{0.3}Co_4Sb_{12}$ sample decreased by about 20% after accelerated thermal aging tests for 15 days. The σ of the sample with Al coating decreased about 15–20%. However, the σ of the samples coated with Al-Ni or Al-Ni-Al coating were almost unchanged after accelerated thermal aging because the sublimation of antimony and oxidation were effectively suppressed. Figure 8b and c shows that the Seebeck coefficient and κ of all samples have little difference after the accelerated thermal aging. The changes are within the range of testing error. From the measured electrical and thermal properties, the ZT values of $Yb_{0.3}Co_4Sb_{12}$ samples coated with different coatings can be calculated. In Fig. 8d, we see that the ZT of the uncoated $Yb_{0.3}Co_4Sb_{12}$ sample after accelerated thermal aging tests for 15 days was decreased by about 20%. This is mainly caused by the decline of electrical conductivity. The ZT value of the sample with Al coting decreased about 18%. Comparing the ZT values between the uncoated sample and the Al-coated sample, it can be concluded that Al coating in this work has little effect on protecting the $Yb_{0.3}Co_4Sb_{12}$ sample. However, the ZT values of the $Yb_{0.3}Co_4Sb_{12}$ samples coated with Al-Ni and Al-Ni-Al were almost unchanged after accelerated thermal aging testing for 15 days, confirming their effectiveness in inhibiting the oxidation and the sublimation of Sb. Considering the cost of the preparation for coating and to simplify the preparation process, the Al-Ni coating is the optimal one

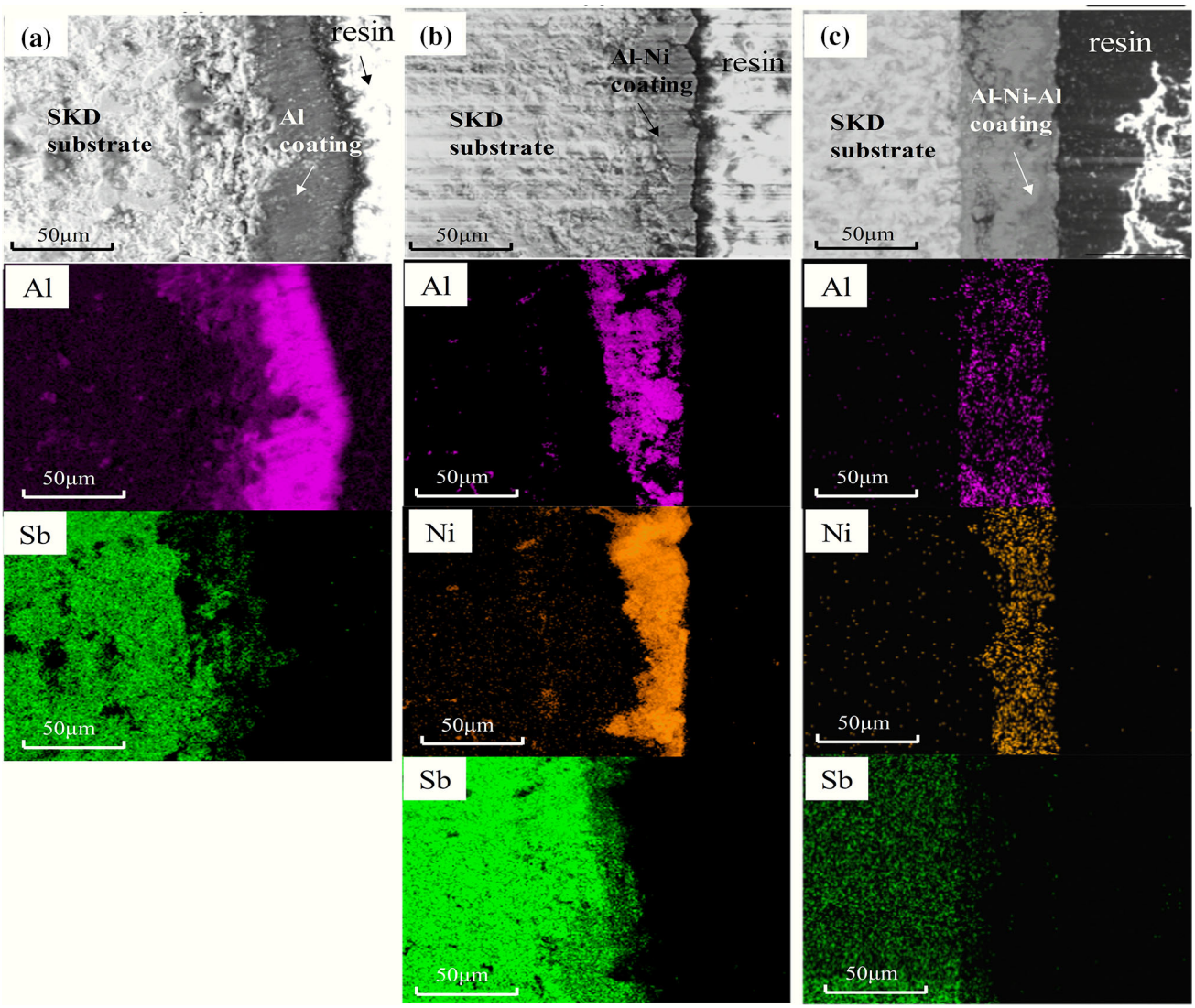

Fig. 6. SEM images and concentration profiles of the Al, Ni and Sb elements in the cross-section of different coatings on $Yb_{0.3}Co_4Sb_{12}$ substrate using DC electrochemical deposition after thermal-aging at 873 K for 15 days. (a) Al coating, (b) Al-Ni coating, (c) Al-Ni-Al coating.

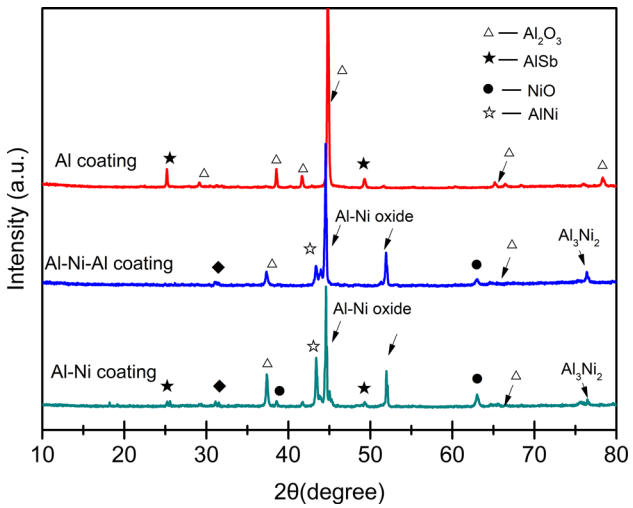

Fig. 7. XRD patterns of the different coatings on $Yb_{0.3}Co_4Sb_{12}$ substrate after thermal aging at 873 K for 15 days.

Table IV. The contents of Al-Ni diffusion layer analysis by EDS technology

$AlNi_3$	40%
Al_2Ni_5	35%
AlNi	5%
Al-Ni oxidation	20%

for protecting $Yb_{0.3}Co_4Sb_{12}$ from oxidation and sublimation of Sb.

According to these results, the thermal aging tests mainly affect the electrical conductivity of $Yb_{0.3}Co_4Sb_{12}$. In order to adequately verify the protective effect of Al-Ni coatings on the substrate, we conducted the accelerated thermal aging test at 873 K on the $Yb_{0.3}Co_4Sb_{12}$ samples with Al-Ni coating for 5 days, 10 days, 15 days and 30 days. The thermal aging test was also carried out in an air

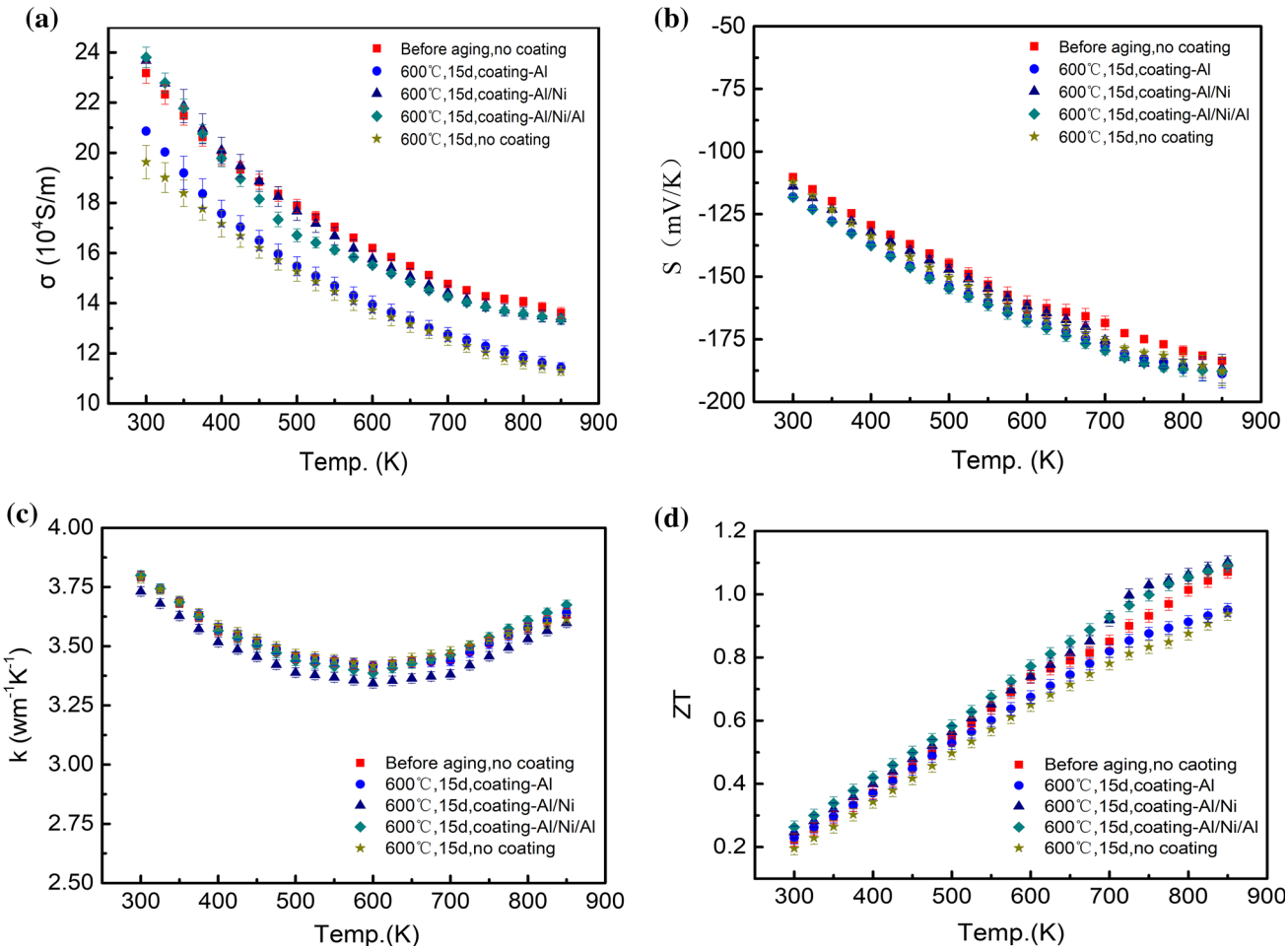

Fig. 8. Thermoelectric properties of the $Yb_{0.3}Co_4Sb_{12}$ samples coated with different coatings after 873 K-thermal aging for 15 days. (a) electrical conductivity, (b) Seebeck coefficient, (c) thermal conductivity, (d) dimensionless figure of merit, *ZT*.

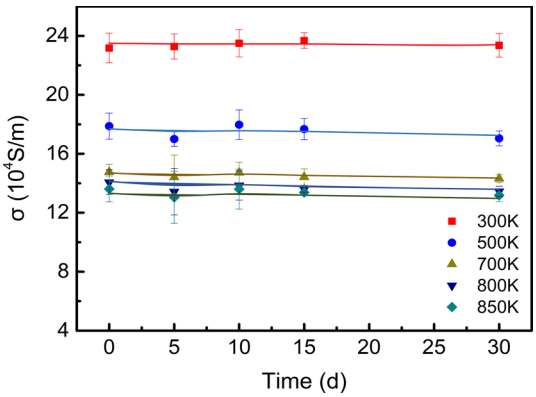

Fig. 9. Electrical conductivity of Al-Ni coated $Yb_{0.3}Co_4Sb_{12}$ sample after 873 K-thermal aging under different times.

atmosphere. As is shown in Fig. 9, the σ of $Yb_{0.3}Co_4Sb_{12}$ samples coated with Al-Ni coating showed little change after the 873 K-thermal aging. With the extension of the aging time, the σ values measured at 300 K, 500 K, 700 K, 800 K and 850 K all remain stable. Therefore, the Al-Ni coating deposited by DC electroplating technique is definitely qualified for suppressing the oxidation and the sublimation of Sb for $Yb_{0.3}Co_4Sb_{12}$-based skutterudite.

CONCLUSIONS

Three kinds of protective coatings of Al, Al-Ni and Al-Ni-Al were successfully deposited onto $Yb_{0.3}Co_4Sb_{12}$ substrates by a DC electroplating technique. The sole Al coating looks like a reticulation with lots of micropores. An interlayer identified as $CoSb_2O_4$ is generated between the Al coating and $Yb_{0.3}Co_4Sb_{12}$ after thermal aging tests in air due to the loose structure of the Al coating, which results in a failure to protect the $Yb_{0.3}Co_4Sb_{12}$ from oxidation. On the other hand, Al and Ni in the Al-Ni or Al-Ni-Al coatings diffuse mutually during the thermal aging tests, forming an ordered fine-grained structure within the original coatings, effectively preventing the oxidation of skutterudite and the sublimation of Sb. Compared to the samples without coating or coated only with Al, the stability of thermoelectric properties of the samples coated with Al-Ni or Al-Ni-Al was significantly improved. The *ZT* values for Al-Ni or Al-Ni-Al coated samples are

almost unchanged after thermal aging at 873 K for 30 days in air. Considering the preparation process, the Al-Ni coating is regarded as a suitable coating for preventing the oxidation of $Yb_{0.3}Co_4Sb_{12}$ and suppressing the sublimation of antimony.

ACKNOWLEDGMENTS

This work was supported by National Natural Science Foundation of China (NSFC) under the Nos. 51676117, 51406111 and 51572282, Shanghai Polytechnic University Graduate Program Foundation No. EGD17YJ0036.

REFERENCES

1. J. Zhang, B. Xu, F. Yu, D. Yu, Z. Liu, J. He, and Y. Tian, *J. Alloys Compd.* 503, 490 (2010).
2. L. Zhang, N. Melnychenko-Koblyuk, E. Royanian, A. Grytsiv, P. Rogl, and E. Bauer, *J. Alloys Compd.* 504, 53 (2010).
3. Z. Xiong, X. Chen, X. Huang, S. Bai, and L. Chen, *Acta Mater.* 58, 3995 (2010).
4. X. Shi, J. Yang, J.R. Salvador, M. Chi, J.Y. Cho, H. Wang, S. Bai, J. Yang, W. Zhang, and L. Chen, *J. Am. Chem. Soc.* 133, 7837 (2011).
5. G. Rogl, A. Grytsiv, P. Rogl, N. Peranio, E. Bauer, M. Zehetbauer, and O. Eibl, *Acta Mater.* 63, 30 (2014).
6. P. Qiu, X. Xia, X. Huang, M. Gu, Y. Qiu, and L. Chen, *J. Alloys Compd.* 612, 365 (2014).
7. D. Zhao, C. Tian, S. Tang, Y. Liu, L. Jiang, and L. Chen, *Mater. Sci. Semicond. Process.* 13, 221 (2010).
8. Q. Zhang, X. Huang, S. Bai, X. Shi, C. Uher, and L. Chen, *Adv. Eng. Mater.* 18, 194 (2016).
9. M.S. El-Genk, H.H. Saber, T. Caillat, and J. Sakamoto, *Energy Convers. Manage.* 47, 174 (2006).
10. H.H. Saber and M.S. El-Genk, *Energy Convers. Manage.* 48, 1383 (2007).
11. E. Godlewska, K. Zawadzka, K. Mars, R. Mania, K. Wojciechowski, and A. Opoka, *Oxid. Met.* 74, 205 (2010).
12. D. Zhao, M. Zuo, Z. Wang, X. Teng, and H. Geng, *Appl. Surf. Sci.* 305, 86 (2014).
13. H. Dong, X. Li, Y. Tang, J. Zou, X. Huang, Y. Zhou, W. Jiang, G. Zhang, and L. Chen, *J. Alloys Compd.* 527, 247 (2012).
14. H. Dong, X. Li, X. Huang, Y. Zhou, W. Jiang, and L. Chen, *Ceram. Int.* 39, 4551 (2013).
15. X. Zhao, X. Shi, L. Chen, W. Zhang, S. Bai, Y. Pei, X. Li, and T. Goto, *Appl. Phys. Lett.* 89, 1325 (2006).
16. Z. Yao, X. Li, Y. Tang, and L. Chen, *J. Electron. Mater.* 44, 1890 (2015).
17. J. Leszczynski, K. Wojciechowski, and A. Malecki, *J. Therm. Anal. Calorim.* 105, 211 (2011).
18. D. Zhao, C. Tian, Y. Liu, C. Zhan, and L. Chen, *J. Alloys Compd.* 509, 3166 (2011).
19. X. Xia, P. Qiu, X. Shi, X. Li, X. Huang, and L. Chen, *J. Electron. Mater.* 41, 2225 (2012).
20. H. Natter and R. Hempelmann, *Electrochim. Acta* 49, 51 (2004).
21. H. Okamoto, *J. Phase Equilib.* 14, 257 (1993).
22. R. Arroyave, D. Shin, and Z.K. Liu, *Acta Mater.* 53, 1809 (2005).
23. L. Battezzati, P. Pappalepore, F. Durbiano, and I. Gallino, *Acta Mater.* 47, 1901 (1999).